International Journal of Creative and Open Research in Engineering and Management
ISSN: 3108-1754 (Online)
Volume 02 Issue 09 September-2026 | Impact Factor: 3.5

Composed Integral Kernels, Fractional Cell Dynamics, and Multi-Scale Resilience in Electrified Mobility Networks

[1]A. A. Gupta, [2]S. M. Shinde
[1]Research Scholar, [2]Prof, Department of Mathematics
Government College of Engineering, Amravati, Maharashtra, India

How to Cite this Article:

Gupta, A. A. (2026). Composed Integral Kernels, Fractional Cell Dynamics, and Multi-Scale Resilience in Electrified Mobility Networks. International Journal of Creative and Open Research in Engineering and Management, <i>02</i>(9), 1-9. https://doi.org/10.55041/ijcope.v2i9.070

https://doi.org/10.55041/ijcope.v2i9.070

Abstract—
Electrified mobility couples electrochemical cells, thermal envelopes, power electronics, and logistics networks whose time scales differ by several orders of magnitude. Integer-order Thevenin circuits under-represent mid-band impedance of lithium-ion cells, while purely discrete event models of supply chains under-represent continuous residue structure that appears after a disruption. This note develops a single theoretical thread: a composed Laplace–Weierstrass kernel acting on a two-parameter test space, a Caputo–Thevenin plant with constant-phase branches, a residue calculus for multi-scale hybrid-vehicle and inventory traces, and a resilience index that a digital replica and a quantum annealer can both read. Battery sizing rules for plug-in architectures, solar-assisted energy balances, smart-mobility constraints, and ledgered event traces are treated as boundary data for the same operators rather than as disconnected application silos. The development is strictly theoretical: existence of the composed transform, well-posedness of the fractional electro-thermal system, spectral extraction of resonant modes, and variational form of unit-load configuration under disruption.

Keywords: Laplace–Weierstrass composition; two-sided FKF transform; Caputo CPE; electro-thermal Thevenin; SoC/SoH; residue resonance; supply-chain resilience; digital twin; quantum annealing; solar-assisted mobility.

I. INTRODUCTION

Plug-in hybrid architectures force a joint choice of traction-battery energy, power capability, and thermal headroom long before a cell-level observer is designed, and that joint choice already encodes the duty cycle that later appears as the current i(t) of a fractional plant. Early Formula Hybrid sizing arguments treat pack energy as an integral of a prescribed speed–grade profile against a conversion efficiency map [11], which is precisely the data that a later Coulomb-count state will integrate. Materials and management reviews of automotive cells then supply the temperature-dependent maps R0(T,z), Q(T,z) and the open-circuit surface Uoc(z,T) that close the electrical–thermal loop [14], [15]. Smart-mobility service constraints [16] and solar-assisted auxiliary power [17] change the sign and the spectrum of i(t), so the same cell is not identified under a single excitation class.

A second axis is organizational rather than electrochemical. Global supply networks that feed cells, packs, and charging assets are subject to internal complexity (inventory position, state of charge of buffer stores) and external complexity (lead-time shocks, climate, regulatory switches) [23], [24]. Resilience reviews and systematic maps of digital-transformation practice argue that a replica of the physical flow, an auditable event ledger, and a combinatorial reallocation engine must share a common state language [22], [25]. The present note takes that language to be the same test-function space on which a two-sided FKF transform is sequentially convergent [29], so that a time shift in a logistics trace [28] and a fractional derivative in a polarization voltage are dual operations rather than metaphors.

Scope of the operators

The operators used below are of three kinds. First, a composed integral transform whose Laplace factor converts polynomial-coefficient dynamics into dual multiplication and whose Weierstrass factor regularizes high-frequency content that EIS and scanrate logistics data both contain. Second, Caputo derivatives of order $\alpha \in (0,1]$ placed on each constant-phase branch of a Thevenin circuit, because a depressed Nyquist arc is the frequency signature of a CPE and not of an ideal capacitor. Third, a residue projector that extracts resonant poles of a multi-scale spectrum, including hybrid-vehicle load traces and inventory oscillations after a disruption. Quantum annealing enters only as a solver for a quadratic unconstrained binary form of unit-load configuration; it does not replace the analytic kernel.

Standing hypotheses

Throughout, currents are locally integrable, temperatures remain in a compact interval on which parameter maps are Lipschitz, and test functions vanish with all derivatives at the temporal boundary used by Caputo's definition. Capacity Qn and coulombic efficiency η are treated as slowly varying relative to the electrical time constants, which licenses a two-time-scale split between SoC kinematics and polarization. No claim is made that an embedded battery-management unit must implement the long Grünwald–Letnikov kernel; the analysis is existence and structure, not firmware.

II. OPERATIONAL CALCULUS OF THE COMPOSED KERNEL

Sequential convergence on the two-sided FKF testing space is the analytic reason a time-shift in a supply-chain trace remains inside the same dual algebra that a fractional cell model uses [29]. Let a > 0 and A, B > 0 be fixed. The space consists of all infinitely differentiable maps (t, y) whose seminorms remain finite for every multi-index of time derivatives, spatial derivatives, and polynomial weights. The constants in those seminorms depend on the test function and not on a particular trajectory of current or inventory.

$$p_{\mathrm{k,l,q}}(\varphi) \;=\; \sup \left| t^{k} e^{\mathrm{A}t}\, \partial_t^{l}\, \partial_y^{q}\, \varphi \right|$$

Multiplication by time t on the Laplace side and differentiation with respect to t interchange under the composed kernel. For functions vanishing at t = 0−, or carrying a known initial value, the first-order rules read as follows.

$$\mathcal{L}\{\, \mathrm{t}\, \varphi(\mathrm{t}) \,\} \;=\; -\mathrm{d_s}\, \Phi(\mathrm{s})$$
$$\mathcal{L}\{\, \varphi'(\mathrm{t}) \,\} \;=\; \mathrm{s}\, \Phi(\mathrm{s}) \;-\; \varphi(0_{-})$$

Higher powers follow by induction. Time differentiation maps to multiplication by powers of the dual variable, and multiplication by powers of the independent variable maps to differentiation in the dual variable. These two families convert linear differential or delay equations with polynomial coefficients into purely algebraic or lower-order dual equations. An expanded treatment of the time-shift property of the FKF transform shows that a delay τ in a logistics release map becomes a multiplier $e^{-s\tau}$ after composition [28], which is the same factor that a delayed thermal measurement would produce on the cell side.

$$\mathcal{L}\{\, \varphi(\mathrm{t} \,-\, \tau) \,\} \;=\; e^{-s\tau}\, \Phi(\mathrm{s}), \quad \tau \,\geq\, 0$$

Weierstrass regularization and the composed symbol

The Weierstrass factor is the Gauss kernel acting in an auxiliary variable y. Its role is to restore rapid decay in the dual variable when the Laplace image of a CPE, which behaves as s^{α} at infinity only in a sector, would otherwise leave the test space. The composed symbol is therefore a product.

$$\mathrm{K}(\mathrm{s}, \xi) \;=\; e^{-\mathrm{B}\xi^2} \cdot \frac{1}{s^{\alpha}}$$

Sequential convergence in that space means that if φn → φ in every seminorm, then the composed images converge in the dual seminorms. That statement is what licenses term-by-term inversion of a truncated Grünwald–Letnikov series and term-by-term extraction of residues from a spectral trace of a hybrid-vehicle powertrain. Without it, a finite memory length L would be an uncontrolled projection rather than a consistent Galerkin cut.

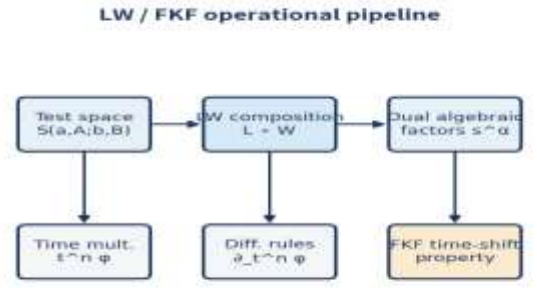

Figure. Flow of the Laplace–Weierstrass composition from the test space to dual algebraic factors and the FKF time-shift.

Caputo placement inside the same algebra

A CPE impedance ZCPE(jω) = 1/(Q (jω)$^{\alpha}$) is the boundary value of 1/(Q s^{α}). Caputo's derivative of order α is preferred for control-oriented models because initial conditions remain ordinary traces v(0), $\dot{v}(0)$, … rather than fractional integrals of the history.

$$\mathrm{D}_t^{\mathrm{C}\alpha}\mathrm{f(t)} \;=\; \frac{1}{\Gamma(n \,-\, \alpha)} \int_0^{t} (t \,-\, \tau)^{n\,-\,\alpha\,-\,1} f^{(\mathrm{n})}(\tau)\, \mathrm{d}\tau$$

The discrete Grünwald–Letnikov form used in most estimation papers is a consistent Riemann-sum realization of the same operator when the memory length L tends to infinity inside the test space.

$$\mathrm{D}_t^{\mathrm{GL}\alpha} v_k \;\approx\; \mathrm{T}_s^{-\alpha} \sum_{\mathrm{j}\,=\,0}^{\mathrm{L}} (-1)^{j}\, \frac{\Gamma(\alpha \,+\, 1)}{\Gamma(j \,+\, 1)\, \Gamma(\alpha \,-\, j \,+\, 1)}\, v_{k\,-\,j}$$

International Journal of Creative and Open Research in Engineering and Management
ISSN: 3108-1754 (Online)
Volume 02 Issue 09 September-2026 | Impact Factor: 3.5

III. FRACTIONAL ELECTRO-THERMAL CELL DYNAMICS

Automotive battery reviews collect the empirical fact that a mid-frequency Nyquist plot of a lithium-ion cell is a depressed semicircle followed by a near-forty-five-degree tail [14], [15], which is the geometry of constant-phase elements and not of ideal capacitors. Replacing each capacitor by a CPE is therefore the circuit-level expression of that geometry. Pack-level sizing for plug-in hybrids supplies the amplitude of i(t) against which the CPE voltages must remain inside a voltage window [11]; solar-assisted architectures add a slowly varying photovoltaic current that shifts the mean of i(t) without restoring integer-order dynamics [17].

First-order fractional Thevenin plant

The terminal voltage and the Caputo polarization branch are written as follows.

$$v_t(\mathrm{t}) = U_{\mathrm{oc}}(\mathrm{z},\mathrm{T}) + R_0\,\mathrm{i}(\mathrm{t}) + v_p(\mathrm{t})$$

$$\mathrm{D}_t^{\mathrm{C}\alpha} v_p = -\frac{1}{R_1 Q} v_p + \frac{1}{Q}\mathrm{i}$$

SoC kinematics remain integer-order Coulomb counting because capacity is an extensive stored charge, not a CPE.

$$\dot{\mathrm{z}} = -\frac{\eta}{Q_n}\mathrm{i}$$

Second-order topology and Warburg tail

Two CPEs, typically with α1 near the charge-transfer depression and α2 near one half for diffusion, give the workhorse plant of SoC papers.

$$v_t = U_{\mathrm{oc}} + R_0\mathrm{i} + v_1 + v_2$$

$$\mathrm{D}_t^{\mathrm{C}\alpha_k} v_k = -\frac{v_k}{R_k Q_k} + \frac{i}{Q_k},\ \mathrm{k} = 1, 2$$

A series Warburg or finite-space Warburg extends the low-frequency tail. Heavier ladders do not automatically improve an observer once identification noise is admitted: R(RQ) or R(RQ)W often dominate once α and Q are recognized as correlated. Variable-order maps α = α(z) track a changing diffusion regime across a wide SoC window at the price of a map that is difficult to identify online. Physics-informed reductions of a single-particle model keep order one half because spherical diffusion in a particle is of that order.

Lumped thermal envelope

Polarization heat and ohmic heat feed a single energy balance on the cell mass. The open-circuit surface Uoc remains a nonlinear lookup or polynomial in SoC and temperature, as required by hybrid-pulse-power characterization.

$$\mathrm{m}\,c_p\,\dot{\mathrm{T}} = \mathrm{i}(v_t - U_{\mathrm{oc}}) + \frac{T}{U_{\mathrm{oc}}}\frac{\partial U_{\mathrm{oc}}}{\partial T}\,\mathrm{i} - \mathrm{hA}(\mathrm{T} - T_{\mathrm{amb}})$$

Electrical parameters R0(T,z), Q(T,z), α(T) are temperature maps. Asynchronous identification is natural at low temperature because thermal and electrical time scales separate. A joint fractional Kalman filter then estimates SoC and surface temperature together. Drive-cycle excitation by WLTP Class-3 and US06 at one to ten hertz is the standing numerical laboratory for the coupled DAE.

Observers and health features

The discrete GL sum folds into the process model of an FO-EKF, FO-AEKF, or FO-UKF. Sliding-mode and particle filters exist but are less common on embedded hardware. Voltage residuals fall relative to an integer Thevenin plant with the same filter because the mid-band geometry is no longer structurally biased. SoC kinematics are unchanged; the gain comes from a cleaner innovation. The CPE exponent α and the admittance Q drift with SEI growth and particle cracking, so they are admissible SoH coordinates if they are estimated on a slower clock than SoC. No fractional electrical model repairs a defective Uoc table: the fractional part only cleans overpotential.

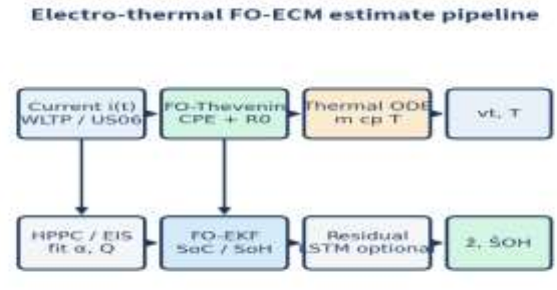

Figure. Electro-thermal FO-ECM path from drive-cycle current through CPE dynamics and a fractional observer to SoC and SoH.

IV. SPECTRAL RESIDUES ACROSS VEHICLE-SUPPLY SCALES

Hybrid-vehicle power and inventory position after a disruption are both multi-scale signals. A residue-based extractor isolates poles that persist when the composed kernel is applied, which is the content of spectral analysis for multi-scale supply-chain dynamics in hybrid-vehicle systems. The same FKF time-shift that aligned delayed thermal samples now aligns delayed shipment releases.

Residue projector

Let Ψ(s) be the composed image of a scalar trace ψ(t) (pack power, warehouse occupancy, or charger occupancy). Isolated poles sk of finite multiplicity mk contribute residues

$$Res_{s=s_k}\,\Psi = \frac{1}{(m_k-1)!}\,lim_{s\to s_k}\,\partial^{(m_k-1)}\left[(s-s)^{m_k}\,\Psi(s)\right]$$

A practical numerical form replaces the limit by a contour integral of small radius on which the Weierstrass factor has already killed the essential spectrum at infinity. Resonant modes of a hybrid powertrain under a repeated urban cycle then sit next to resonant modes of a replenishment policy, and both can be tracked as slow features for resilience scoring.

$$Res_k = \frac{1}{2\pi i}\oint_{\Gamma_k}\Psi(s)\,ds$$

Alignment by time shift

When two traces differ by a release delay τ, the FKF shift multiplies the dual image by $e^{\{-s\tau\}}$. Residue locations are invariant; only the complex argument of the residue rotates. That invariance is what permits a warehouse trace and a pack-power trace to be compared after a logistics lag without re-identifying the pole set. Sequential convergence of the two-sided testing space guarantees that a truncated Fourier–Laplace series of the trace still sees the same poles. Spectral work on hybrid-vehicle and chain traces already isolates those poles as operational features [18], and the two-sided testing-space result [29] is what makes the truncation legitimate rather than heuristic.

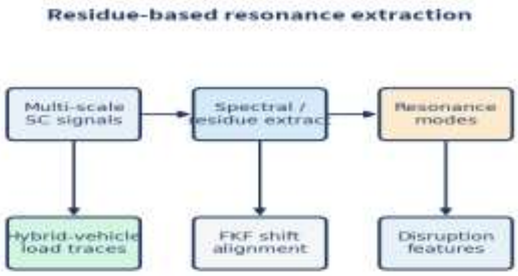

Figure. Residue extraction from multi-scale supply and hybrid-vehicle traces after FKF alignment.

V. RESILIENCE ARCHITECTURES AND DIGITAL REPLICAS

Resilience of a global chain that feeds cells and charging assets is not a single scalar reliability. Reviews of internal and external complexity treat inventory, conversion capacity, and information delay as internal coordinates, and treat geopolitical, climatic, and regulatory shocks as external coordinates. Digital-transformation surveys add a replica that must stay consistent with both. The present construction reads those coordinates through the same composed kernel, so a shock is a jump in a test function rather than a separate narrative layer.

A working resilience index

Let xin collect internal states (SoC of buffer packs, on-hand inventory, charger availability) and let ξex collect exogenous intensities. A simple Lipschitz index is

$$\mathcal{R}(t) = \exp\left(-\int_0^t \lambda(x_{in}, \xi_{ex})\,d\sigma\right)$$

The rate λ is assembled from residue amplitudes of the traces in Section IV and from voltage-window violations of the cell plant in Section III. Anti-theft power-line carrier links [12] and swipe-style access controllers [13] enter only as integrity constraints on the event stream that updates xin: if the stream is spoofed, the replica diverges and $\mathscr{R}$ is no longer a function of the physical plant.

Replica consistency and ledgered events

A digital twin of a chain is consistent when the push-forward of the physical measure under the composed kernel stays within a prescribed dual ball of the replica measure. Artificial-intelligence layers that propose reallocations [20], and distributed ledgers that timestamp those reallocations [21], act on events rather than on the kernel itself. Transparency and traceability therefore constrain the admissible event σ-algebra; they do not alter Caputo order or residue locations. Green-logistics bibliometric structure [20] is used here only to name the exogenous intensities that most often appear in λ: carbon price, last-mile congestion, and renewable-generation intermittency that also drives the solar-assisted current of Section III.

$$\| \mathcal{K}\mu_{phys} - \mathcal{K}\mu_{twin} \|_* \le \varepsilon$$

Figure. Internal and external coordinates feeding a resilience index through a digital replica and an auditable event layer.

VI. QUANTUM AND LEARNING LAYERS FOR RECONFIGURATION

Once a disruption has moved residue amplitudes and the replica has accepted the new measure, the remaining task is combinatorial: re-pack unit load devices, re-assign routes, and re-split charging slots. Quantum-annealing maps of unit-load configuration [27] write that task as an Ising energy whose ground state is a feasible packing. Learning residual correctors, already used to eat structured voltage error after a fractional Kalman step, can equally eat structured forecast error after an anneal.

Ising form of unit-load configuration

Binary variables si ∈ {−1, +1} encode assignment of a shipment to a device. Couplers Jij encode volume, mass, and hazardous-separation constraints; fields hi encode priority and delay-cost after the shock.

$$H(s) = \sum_{i<j} J_{ij} s_i s_j + \sum_i h_i s_i$$

Practical logistics surveys of the quantum stack [19], [26] treat annealing as a hybrid inner loop: a classical outer heuristic proposes a reduced coupler graph, the annealer returns a low-energy sample, and a classical repair restores hard constraints that the Ising penalty only softly encoded. Disruption scenarios generated from the residue model of Section IV supply the fields hi, which is the only coupling back to the analytic kernel.

Residual learners beside the plant

A lean FO-ECM plus a small learned residual is preferable to growing a third CPE. The same pattern applies to logistics: the Ising energy plus a small Gaussian-process correction on delay, rather than an ever larger coupler graph. On electrical traces the published pattern is that an FO+UKF residual fed to a short LSTM reduces SoC error on US06 and FUDS without touching SoC kinematics. On logistics traces the analogous statement is that a short residual on travel time reduces the realized energy of H without retuning Jij.

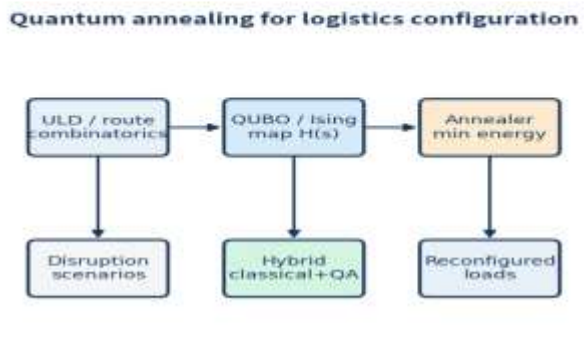

Figure. Map from combinatorial logistics state through a QUBO/Ising energy to an annealed reconfiguration, with disruption fields from the residue model.

Well-posedness sketch for the coupled plant

Caputo's operator on a Banach-valued path with locally integrable forcing admits a unique mild solution when the linear symbol $-1/(R_k Q_k)$ is sectorial of angle less than (1 − α/2)π. The thermal ODE is Lipschitz in (v_t, T) on the compact temperature interval assumed in Section I, so a short-time contraction in C([0, t*]; $R^{\{2+n\}}$ extends globally while voltage remains in a window compatible with pack sizing [11]. Solar-assisted mean current [17] enters as a slowly varying parameter of that forcing and does not change the sector.

$$v_k(t) = E_\alpha\left(-\frac{t^\alpha}{R_k Q_k}\right) v_k(0) + \int_0^t (t - \sigma)^{\alpha-1} E_{\alpha,\alpha}\left(-\frac{(t-\sigma)^\alpha}{R_k Q_k}\right) \frac{i(\sigma)}{Q_k}\, d\sigma$$

Here E_α and $E_{\alpha,\alpha}$ are Mittag–Leffler kernels. The same variation-of-constants formula is what an FO-EKF linearizes at each step. Smart-mobility schedules [16] change i only through a bounded measurable map, so the mild solution remains in the test space on which sequential FKF convergence was stated [29].

Event integrity as a constraint, not a dynamics

Power-line carrier anti-theft signalling [12] and swipe authentication [13] restrict the admissible event stream that updates internal coordinates of the resilience index. They do not appear in the Caputo symbol or in the Ising coupler graph. If the stream is inconsistent with the replica ball of Section V, the correct response is to freeze reallocation rather than to retune α. Artificial-intelligence recommenders [20] and ledgered timestamps [21] likewise act after the kernel, which keeps the analytic estimates independent of a particular vendor stack.

Digital-twin surveys [22] and digital-transformation agendas [25] already insist on that separation: the replica is a measure push-forward, the recommender is a policy on events, the ledger is an audit of that policy. Weaving internal and external complexity [24] then reduces to keeping λ in the resilience index Lipschitz in both blocks. Green-logistics intensities drawn from bibliometric maps [20] only name the most frequent external coordinates; they are not additional operators.

VII. OPEN LINES OF INQUIRY

Short-memory Caputo recurrences that a thirty-two-bit management unit can evaluate at ten hertz remain an implementation gap, not a theorem gap. Joint identifiability of α(z, T, SoH) without overfitting is the corresponding statistical gap. Physics-reduced fractional circuits whose states remain concentrations and overpotentials would reconnect the CPE exponent to spherical diffusion rather than to a free fit. Below freezing the diffusion order itself moves, so an electro-thermal model with a state-dependent α is still open. On the network side, sequential convergence of the two-sided FKF space under measure-valued inventory processes is not yet written, and neither is a certified bound that would tell an annealer when a residue shift is large enough to justify a full re-pack.

Battery-technology reviews continue to stress that mid-frequency health features are under-used in production estimators [15], while sizing practice still treats the pack as an energy integral against a prescribed cycle [11]. The present operators give those two facts a common dual variable: the CPE exponent lives in the same s-plane as the residue of a delayed replenishment [28]. Quantum-transport surveys [19] and logistics-annealing notes [26], [27] then read that plane only through the fields of an Ising energy. Nothing in that chain requires a third CPE or a larger test-space seminorm.

Three concrete developments follow the existing operators. The first is a discrete FO-Thevenin plus FO-EKF written so that every matrix entry is a GL coefficient or a Caputo two-step weight. The second is a controlled comparison of one-CPE, two-CPE, and R(RQ)W plants on a public cell archive, with EIS-fitted α held fixed while time-domain observers run. The third is a coupling of the fractional electrical plant to the lumped thermal ODE already stated, under a solar-assisted current that is itself the output of a smart-mobility schedule.

VIII. CONCLUSION

A composed Laplace–Weierstrass kernel, a Caputo–Thevenin cell with thermal closure, a residue projector on hybrid-vehicle and inventory traces, and an Ising reallocation layer can be written in one algebraic setting. Integer dual-polarization circuits remain the rational embedded default wherever memory, sample rate, and validation cost dominate. Fractional plants earn their parameters when mid-band impedance, low-temperature diffusion, or aging-sensitive CPE coordinates are the object. Digital replicas and annealers earn their cost when residue shifts after a shock are large enough that a local heuristic cannot restore feasibility. The theory does not collapse those layers into one algorithm; it only shows that they act on a common test space and a common dual symbol.

What remains is not a larger narrative but a shorter list of estimates: a memory length that does not bias Caputo order, a residue contour that does not pick the essential spectrum, and a coupler graph small enough that an annealer's sample is a feasible pack. Those estimates belong to computation. The operators that make them comparable belong to the composed kernel.

REFERENCES

1. S. M. Harle, "Artificial Intelligence-Based Pavement Crack Detection: A Comprehensive Review of Machine Learning and Deep Learning Techniques," Int. Res. J. Modernization Eng. Technol. Sci., vol. 8, pp. 50–69, Jan. 2026.
2. S. M. Harle, "Digital Twins and Artificial Intelligence for Sustainable Textile Raw Material Processing," Int. Res. J. Modernization Eng. Technol. Sci., vol. 8, pp. 14–30, Jan. 2026.
3. Ivanov, D., Dolgui, A., & Sokolov, B. (2019). The impact of digital technology and Industry 4.0 on the ripple effect and supply chain risk analytics. *International Journal of Production Research*, 57(3), 829–846.
4. Ivanov, D. (2021). Digital supply chain twins: Managing the ripple effect, resilience, and disruption risks by data-driven optimization, simulation, and visibility. In *Handbook of Ripple Effects in the Supply Chain* (pp. 309–330). Springer.
5. V. D. Sharma and A. N. Rangari, "Operational Calculus on Generalized Fourier-Laplace Transform," *International Journal of Scientific and Innovative Mathematical Research*, vol. 2, no. 11, pp. 862–867, 2014.
6. V. D. Sharma, "Operational Calculus on Generalized Two-Dimensional Fractional Fourier Transform," *International Journal of Engineering and Innovative Technology*, vol. 3, no. 2, pp. 253–256, 2013.
7. V. D. Sharma and P. B. Deshmukh, "Inversion Theorem of Two Dimensional Fractional Fourier-Mellin Transform," *International Journal of Applied Computational Science & Mathematics*, vol. 4, no. 1, pp. 17–24, 2014.
8. V. D. Sharma and P. B. Deshmukh, "Generalized Two-Dimensional Fractional Mellin Transform," *Proceedings/IEEE*, pp. 900–903.
9. V. D. Sharma and P. B. Deshmukh, "S-Type Spaces for Two Dimensional Fractional Fourier-Mellin Transform," *International Journal of Advances in Science, Engineering and Technology*, pp. 74–76, June 2015.
10. V. D. Sharma and P. B. Deshmukh, "Topological Properties of Two Dimensional Fractional Fourier-Mellin Transform," *International Journal of Science, Technology & Management*, vol. 4, Special Issue 1, 2015.
11. A. Gulhane and A. Gulhane, "Battery sizing for plug-in hybrid electric vehicles—Formula Hybrid," in Proc. 2017 IEEE International Conference on Power, Control, Signals and Instrumentation Engineering (ICPCSI), 2017, pp. 368–372, doi: 10.1109/ICPCSI.2017.8392317.
12. A. Gulhane, A. Karale, and C. Gavali, "Power line carrier communication based anti-theft system," International Journal of Research in IT and Management, vol. 4, no. 12, pp. 1–11, 2014. [Online]. Available: https://indianjournals.com/article/ijrim-4-12-001
13. A. Gulhane, A. Karale, and S. Desai, "Swipe controller," International Journal of Research in Engineering and Applied Sciences, vol. 4, no. 12, pp. 1–7,

2014. [Online]. Available: https://indianjournals.com/article/ijreas-4-12-001

14. A. Gulhane, "Advancements in automotive batteries: A review," International Engineering Journal for Research & Development, vol. 8, no. 6, pp. 18–57, 2023. [Online]. Available: https://iejrd.com/index.php/iejrd/article/view/3141

15. A. Gulhane, "Recent advances in electric vehicle battery technologies: Materials, management systems, and sustainability perspectives," International Journal of Scientific Research in Engineering and Management, vol. 9, no. 7, 2025, doi: 10.55041/IJSREM51198.

16. A. Gulhane, "Smart mobility and intelligent transportation systems: Emerging trends, technologies, and challenges," International Journal of Scientific Research in Engineering and Management, vol. 9, no. 11, 2025, doi: 10.55041/IJSREM53436.

17. A. Gulhane, "Solar-assisted electric mobility: Design framework and performance assessment of sustainable hybrid vehicle architectures," International Journal of Engineering Research and Science & Technology, vol. 21, no. 3, pp. 362–368, 2025, doi: 10.56636/ijerst.2025.v21.i03.3594.

18. A. Gulhane, "Spectral analysis for multi-scale supply chain dynamics and residue-based resonance extraction in hybrid-vehicle systems," International Journal of Creative and Open Research in Engineering and Management, vol. 2, no. 8, 2026, doi: 10.55041/ijcope.v2i8.141.

19. A. Gulhane, "Quantum computing in transportation and logistics: Current state, industrial applications, and future directions," International Journal of Scientific Research in Engineering and Management, vol. 9, no. 9, 2025, doi: 10.55041/IJSREM52469.

20. A. Gulhane, "Artificial intelligence applications in sustainable logistics and green supply chain management: A bibliometric review," International Research Journal of Modernization in Engineering Technology and Science, vol. 6, no. 12, 2024, doi: 10.56726/IRJMETS65006.

21. A. Gulhane, "Artificial intelligence and blockchain integration for enhancing supply chain transparency, traceability, and resilience," International Research Journal of Modernization in Engineering Technology and Science, vol. 6, no. 12, 2024, doi: 10.56726/IRJMETS65016.

22. A. Gulhane, "Digital twin technology for building resilient and adaptive global supply chains: A review," International Research Journal of Modernization in Engineering Technology and Science, vol. 6, no. 12, 2024, doi: 10.56726/IRJMETS64992.

23. A. Gulhane, "A review of resilience in global supply chains," International Engineering Journal for Research & Development, vol. 8, no. 4, 2024.

24. A. Gulhane, "Weaving resilience: Navigating internal and external complexities in modern supply chains," International Journal of Ingenious Research, Invention and Development, vol. 3, no. 1, pp. 123–128, 2024, doi: 10.5281/zenodo.11491482.

25. A. Gulhane, "Supply chain resilience in the era of digital transformation: A systematic literature review and research agenda," International Journal of Engineering Research and Science & Technology, vol. 21, no. 4, pp. 1058–1068, 2025, doi: 10.56636/ijerst.2025.v21.i04.3812.

26. A. Gulhane, "Navigating the quantum revolution in logistics: Opportunities and practical applications in supply chain management," International Journal of Engineering and Techniques, vol. 12, no. 3, pp. 553–556, 2026, doi: 10.29126/ijet.2026.v12.i3.553.

27. A. Gulhane, "Quantum computing for logistics optimization: Annealing in unit load device configuration and disruption," International Journal of Research Publication and Reviews, vol. 7, no. 6, pp. 4643–4648, 2026, doi: 10.55248/gengpi.07.0626.16a57.

28. A. Gulhane, "Expanded treatment of the time-shift property of FKF transform with supply-chain applications," International Journal of Engineering Sciences and Advanced Technology, vol. 25, no. 12, pp. 606–616, 2025, doi: 10.64771/ijesat.2025.v25.i12.3817.

29. A. Gulhane, "Sequential convergence in the testing function space of the two-sided FKF transform," International Journal of Creative and Open Research in Engineering and Management, vol. 2, no. 8, 2026, doi: 10.55041/ijcope.v2i8.138.

30. V. D. Sharma and P. B. Deshmukh, "Operational Calculus for Two Dimensional Fractional Fourier-Mellin Transform," *International Journal of Multidisciplinary Research and Development*, vol. 3, no. 1, pp. 99–104, 2016.

31. V. D. Sharma and P. B. Deshmukh, "Analyticity of Two Dimensional Fractional Fourier-Mellin Transform," *International Journal of Engineering Sciences & Research Technology*, 2016, DOI 10.5281/zenodo.47633

32. V. D. Sharma, "Analyticity of Distribution Generalized Fourier-Stieltjes Transforms," 2012.

33. V. D. Sharma, "Operators on the Distributional Generalized Two-Dimensional Fractional Fourier Transform," *International Journal of Modern Mathematical Sciences*, vol. 9, no. 1, pp. 39–45, 2014.